Giant enhancement of the second harmonic generation efficiency in poled multilayered silica glass structures

Ksenia Yadav,[1,*] C. L. Callender,[2] C. W. Smelser,[2] C. Ledderhof,[2] C. Blanchetiere,[2] S. Jacob,[2] and J. Albert[1]

[1]Department of Electronics, Carleton University, 1125 Colonel By Drive, Ottawa, ON, K1S 5B6, Canada
[2]Communications Research Centre, P.O. Box 11490 Station H, Ottawa, ON, K2H 8S2, Canada
*kgolod@doe.carleton.ca

Abstract: Multilayered thin-film doped silica structures are experimentally demonstrated as an effective tool to enhance the second-order nonlinear properties induced in thermally poled glass devices. A 204-fold improvement is obtained in the second harmonic generated (SHG) in a poled structure with a 3 μm-thick multilayered stack consisting of sub-100 nm-thick alternating germanium-doped and undoped silica layers compared to poled bulk silica glass. The induced nonlinearity is localized within the layered region, indicating that the multilayered design can be used to precisely control the thickness and the location of the nonlinearity. Such artificial nonlinear structures can be used to overcome the main limitations of existing poled glass devices, therefore opening the door to practical implementations of efficient active devices in silica glass.

©2011 Optical Society of America

OCIS codes: (190.0190) Nonlinear optics; (160.4330) Nonlinear optical materials; (160.6030) Silica; (310.6845) Thin film devices and applications; (310.4165) Multilayer design; (160.2750) Glass and other amorphous materials.

References and links

1. R. W. Boyd and D. J. Gauthier, "Controlling the velocity of light pulses," Science **326**(5956), 1074–1077 (2009).
2. J. L. O'Brien, A. Furusawa, and J. Vuckovic, "Photonic quantum technologies," Nat. Photonics **3**(12), 687–695 (2009).
3. D. Cyranoski, "Materials science: China's crystal cache," Nature **457**(7232), 953–955 (2009).
4. R. A. Myers, N. Mukherjee, and S. R. J. Brueck, "Large second-order nonlinearity in poled fused silica," Opt. Lett. **16**(22), 1732–1734 (1991).
5. A. C. Liu, M. J. F. Digonnet, and G. S. Kino, "Electro-optic phase modulation in a silica channel waveguide," Opt. Lett. **19**(7), 466–468 (1994).
6. Y. Quiquempois, N. Godbout, and S. Lacroix, "Model of charge migration during thermal poling in silica glasses: evidence of a voltage threshold for the onset of a second-order nonlinearity," Phys. Rev. A **65**(4), 043816 (2002).
7. B.-J. Seo, S. Kim, B. Bortnik, H. Fetterman, D. Jin, and R. Dinu, "Optical signal processor using electro-optic polymer waveguides," J. Lightwave Technol. **27**(15), 3092–3106 (2009).
8. J. Chen, K. F. Lee, X. Li, P. L. Voss, and P. Kumar, "Schemes for fibre-based entanglement generation in the telecom band," New J. Phys. **9**(8), 289 (2007).
9. A. Canagasabey, C. Corbari, A. V. Gladyshev, F. Liegeois, S. Guillemet, Y. Hernandez, M. V. Yashkov, A. Kosolapov, E. M. Dianov, M. Ibsen, and P. G. Kazansky, "High-average-power second-harmonic generation from periodically poled silica fibers," Opt. Lett. **34**(16), 2483–2485 (2009).
10. P. G. Kazansky, A. R. Smith, P. St. J. Russell, G. M. Yang, and G. M. Sessler, "Thermally poled silica glass: laser induced pressure pulse probe of charge distribution," Appl. Phys. Lett. **68**(2), 269–271 (1996).
11. T. G. Alley, S. R. J. Brueck, and R. A. Myers, "Space charge dynamics in thermally poled fused silica," J. Non-Cryst. Solids **242**(2-3), 165–176 (1998).
12. M. Dussauze, V. Rodriguez, A. Lipovskii, M. Petrov, C. Smith, K. Richardson, T. Cardinal, E. Fargin, and E. I. Kamitsos, "How does thermal poling affect the structure of soda-lime glass?" J. Phys. Chem. C **114**(29), 12754–12759 (2010).
13. Q. Liu, B. Poumellec, D. Braga, G. Blaise, Y. Ren, and M. Kristensen, "The change of electric field and of some other insulating properties during isochronal annealing in thermally poled Ge-doped silica films," Appl. Phys. Lett. **87**(12), 121906 (2005).

14. A. Kudlinski, Y. Quiquempois, and G. Martinelli, "Modeling of the $\chi^{(2)}$ susceptibility time-evolution in thermally poled fused silica," Opt. Express **13**(20), 8015–8024 (2005).
15. A. Kudlinski, G. Martinelli, and Y. Quiquempois, "Dynamics of the second-order nonlinearity induced in Suprasil glass thermally poled with continuous and alternating fields," J. Appl. Phys. **103**(6), 063109 (2008).
16. Y. Luo, A. Biswas, A. Frauenglass, and S. R. J. Brueck, "Large second-harmonic signal in thermally poled lead glass-silica waveguides," Appl. Phys. Lett. **84**(24), 4935–4937 (2004).
17. M. Fokine, M. Ferraris, and I. C. Carvalho, "Thermal poling of glass: a nonlinear ionic RC circuit," in *Bragg Gratings, Photosensitivity, and Poling in Glass Waveguides*, OSA Technical Digest (CD) (Optical Society of America, 2007), paper JWBPDP6.
18. W. E. Angerer, N. Yang, A. G. Yodh, M. A. Khan, and C. J. Sun, "Ultrafast second-harmonic generation spectroscopy of GaN thin films on sapphire," Phys. Rev. B **59**(4), 2932–2946 (1999).
19. A. C. Liu, M. J. F. Digonnet, G. S. Kino, and E. J. Knystautas, "Advances in the measurement of the poled silica nonlinear profile," Proc. SPIE **3542**, 115–119 (1998) (Doped Fiber Devices).
20. D. L. Griscom, "Trapped-electron centers in pure and doped glassy silica: a review and synthesis," J. Non-Cryst. Solids **357**(8-9), 1945–1962 (2011).
21. H. An and S. Fleming, "Hindering effect of the core-cladding interface on the progression of the second-order nonlinearity layer in thermally poled optical fibers," Appl. Phys. Lett. **87**(10), 101108 (2005).
22. A. Ozcan, M. Digonnet, G. Kino, F. Ay, and A. Aydinli, "Characterization of thermally poled germanosilicate thin films," Opt. Express **12**(20), 4698–4708 (2004).
23. A. Feltri, S. Grandi, P. Mustarelli, M. Cutroni, and A. Mandanici, "GeO$_2$-doped silica glasses: an ac conductivity study," Solid State Ion. **154–155**, 217–221 (2002).
24. F. C. Garcia, L. Vogelaar, and R. Kashyap, "Poling of a channel waveguide," Opt. Express **11**(23), 3041–3047 (2003).
25. K. Yadav, C. W. Smelser, S. Jacob, C. Blanchetiere, C. L. Callender, and J. Albert, "Simultaneous corona poling of multiple glass layers for enhanced effective second-order optical nonlinearities," Appl. Phys. Lett. **99**(3), 031109 (2011).
26. N. Myrén, H. Olsson, L. Norin, N. Sjodin, P. Helander, J. Svennebrink, and W. Margulis, "Wide wedge-shaped depletion region in thermally poled fiber with alloy electrodes," Opt. Express **12**(25), 6093–6099 (2004).
27. K. Lee, P. Hu, J. L. Blows, D. Thorncraft, and J. Baxter, "200-m optical fiber with an integrated electrode and its poling," Opt. Lett. **29**(18), 2124–2126 (2004).

1. Introduction

Second-order nonlinear crystals are essential for many important applications, including slow light generation [1], optical cryptography [2], frequency doubling, and electro-optic modulation. Although such crystals are widely used, they are difficult to integrate with silica-based optical guiding devices, have substantial damage threshold limitations, and are becoming increasingly difficult to procure around the world [3]. For these reasons it has long been recognized that it would be highly advantageous to find a way to break the inversion symmetry of silica glass and thus induce a second-order nonlinearity in this widely used high-quality optical material. About 20 years ago, it was discovered that thermal poling of silica glass produced such an effect [4]. However, despite the intense research activity that followed, the nonlinear interactions in the demonstrated devices remained too weak for practical applications because of what are now widely accepted fundamental material and process limitations [5, 6]. Here we report a discovery that overcomes these limitations and demonstrate man-made glass structures, which mimic nonlinear crystals and provide a versatile, inexpensive and widely available alternative to natural nonlinear crystals.

The prospect of using silica glass as a second-order nonlinear medium introduces a conceptually different approach to the design of optical systems. In today's optical chips any nonlinear functionality is implemented externally to the chip requiring labor-intensive packaging, or on the chip but using multi-material systems [7] that introduce additional fabrication steps and integration challenges. The monolithic integration of second-order nonlinear functions directly within silica-based optical chips would virtually eliminate any insertion losses, thermal mismatch problems and integration issues, and would be completely compatible with standard planar lightwave circuit (PLC) technology. The idea of a nonlinear silica glass material may also lead to the realization of an efficient second-order nonlinear fiber with very long interaction lengths. Such nonlinear fiber could become a superior alternative to traditionally used crystals (quartz, LBO, KDP, etc.) in a number of prominent applications. For example, it would eliminate coupling losses that degrade the entangled photon pair generation rate in spontaneous parametric down-conversion for quantum cryptography applications [8]. As another example, a nonlinear silica fiber can be spliced

directly with rare-earth doped fiber laser sources to realize rugged and low-cost lasers in the visible frequency range [9]. In all these cases, the properties that make silica glass a key material in integrated and free-space optics—low propagation losses, high optical damage threshold, and a mature and widely available fabrication technology—would also serve as important advantages in nonlinear optical devices.

Nevertheless, silica glass is not generally used in nonlinear optical applications because of its intrinsic inversion symmetry. The amorphous nature of glass implies that its second-order nonlinear coefficient $\chi^{(2)}$ is equal to zero, and the lowest non-zero nonlinear coefficient is of the third order ($\chi^{(3)}$). However, in 1991 a simple process that could break this limitation was discovered [4]. The process, termed *thermal poling*, involves: (1) heating the sample to ~300 °C, (2) applying a high voltage (3–5 kV) across the sample, and (3) cooling the sample to room temperature with the voltage applied. When the sample has cooled and the voltage is switched off, a stable and significant nonlinearity is observed within the glass, with typical second-order susceptibility $\chi^{(2)} \sim 1$ pm/V in silica. This phenomenon is believed to be a consequence of electric field-induced ion migration within the glass [6] illustrated in Fig. 1. The silica glass matrix typically contains impurity alkali ions (such as Na^+ and Li^+) that are bonded to negatively charged non-bridging oxygen sites. However, at elevated temperatures, these ions become mobile, drift away from the anode under the influence of the applied electric field, and leave behind a negatively charged depletion region. In addition, experimental measurements reported a positive charge layer at the anodic surface [10]. When the anode electrode allows contact of the glass with the atmosphere (i.e. it acts as non-blocking electrode), this layer consists of hydrogenated ions (e.g. H^+ or H_3O^+) produced by high field ionization at the glass-anode interface [11]. In the case when the anode prevents the contact of glass with the atmosphere (i.e. the blocking electrode condition), it forms due structural rearrangements and release of non-bridging oxygen atoms within the glass region near the anode [12, 13]. The charge separation between this positive charge layer and the negatively charged depletion region results in a high electric field on the order of 10^7 V/cm. Subsequently, when the sample is cooled, the ions become practically immobile and remain in their new positions even when the voltage is switched off. The electric field E, which becomes frozen in the glass, acts on the intrinsic third-order nonlinearity of the glass $\chi^{(3)}$ to produce an effective second-order nonlinearity $\chi^{(2)}$ proportional to $E\chi^{(3)}$.
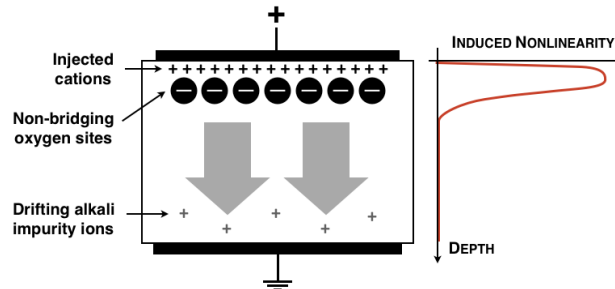

Fig. 1. Charge migration model for the poling-induced second-order nonlinearity in glasses (assuming a non-blocking anode electrode).

Much research has been done to optimize the poling process and to explore different variations of poling, but the nonlinear interactions in resulting devices remained too weak to be used for practical applications. Three main problems have, so far, limited the topic of poled glasses to the realm of research. The first problem is the relatively low value of the induced nonlinear susceptibility coefficient, which has not been significantly improved upon over the initial result of $\chi^{(2)} \sim 1$ pm/V. Although this value is quite far from the strongest tensor element of lithium niobate ($\chi^{(2)}_{33} = 82$ pm/V), it is comparable to the $\chi^{(2)}$ values of other nonlinear crystals that are widely used for frequency doubling (e.g. quartz or KDP). So, in fact, the current value of 1 pm/V is adequate for many practical applications, especially when the long interaction lengths that are possible with silica waveguide- or fiber-based devices are

taken into account. A second and more severe problem with poled glass devices is the difficulty in obtaining high nonlinear susceptibility over thicknesses compatible with standard waveguide or fiber dimensions. On the one hand, in glasses that have a relatively high impurity content (such as Infrasil), where $\chi^{(2)} \sim 1$ pm/V values are routinely obtained, the induced nonlinear region is only ~5 μm thick [4]. This limited extent results in a poor overlap between the nonlinearity and the optical field propagating through the glass, and hence inefficient nonlinear interaction [5]. On the other hand, glasses where the impurity content is much lower (such as Suprasil) do exhibit poling-induced nonlinear regions that span tens of micrometers, but the induced nonlinear effect is an order of magnitude lower than in glasses with higher impurity content [4]. This problem cannot be overcome by poling for longer durations, because a competing detrimental process decreases the poling efficiency for long poling times [14]. In this process, the positive ions that are injected by ionization at the glass-anode interface start moving into the bulk of the sample. Because they are positively charged, they become attracted to the negatively charged non-bridging oxygen sites, and essentially substitute for the impurity alkali ions that have migrated away. This, in turn, reduces the frozen-in electric field and decreases the induced nonlinear effect. The third problem is important from a practical reproducibility standpoint. The impurity levels in bulk silica glasses are typically on the order of a few ppm, and can vary significantly among ingots of nominally identical glass. Because the dynamics of the poling process strongly depend on the impurity content, the extent and the magnitude of the induced nonlinearity are difficult to control [15].

In this work, we present an approach that uses multilayered silica-based structures to alleviate the two latter problems. The rationale behind this approach is that poling-induced second-order nonlinearities often peak at interfaces when deposited glass layers are used [16], possibly due to the accumulation or trapping of charges at interfaces. The use of silica layers, as opposed to homogenous bulk glass, allows a greater control over the migration of charges, and essentially creates a series of nonlinear ionic capacitors [17] that simultaneously participate in the poling process. Therefore, our main hypothesis in this work is that doped silica multilayered structures can be used to control the poling-induced nonlinearity such that a strong nonlinear region is created over a controllable thickness. We demonstrate that poling of multilayered structures involving many thin-film silica layers can be used to obtain more than two orders of magnitude increase in the second harmonic generated (SHG) in the sample compared to the SHG in poled bulk silica glass.

2. Experimental setup

2.1 Thin film deposition

The thin film multilayered structures were deposited by a plasma-enhanced chemical vapor deposition (PECVD) process at 300 °C on 650 μm-thick synthetic fused silica glass substrates (Suprasil 300 by Heraeus). Germane (GeH_4), silane (SiH_4) and nitrous oxide (N_2O) precursor gases were used for the germanium-doped films. The use of nitrous oxide as an oxidizing agent is not expected to have any effect on the poling process, since the nitrogen concentration in the deposited layers was measured to be below the detection limit of energy-dispersive x-ray spectroscopy (EDX) analysis. For proper comparison, all of the samples described in this work were deposited on substrates that were cut from the same ingot to ensure identical impurity content.

2.1 Thermal poling process

The poling was performed at 300 °C in a nitrogen-rich atmosphere. The sample was sandwiched between pressed-on n-type silicon electrodes, and placed on a heater. Homogeneous heat distribution was ensured by keeping the setup at 300 °C for 30 minutes before applying the 3 kV poling voltage across the sample. After the voltage was applied, the temperature was kept at 300 °C for 8 minutes, after which the heater was turned off, and the sample was allowed to cool to room temperature over the course of ~1.5 hours, at which point

the voltage was switched off. For the multilayered samples, the layered side was in contact with the positive electrode.

2.1 Nonlinear characterization method

The nonlinearity induced in the poled samples was characterized by measuring the second harmonic generated in the samples using the Maker fringe method. An ultrafast mode-locked Ti:sapphire laser (operating wavelength 800 nm, pulse width < 70 fsec, repetition rate 80 MHz) was used as the fundamental source. A *p*-polarized beam was focused onto the sample, and the generated second harmonic signal was measured as a function of incidence angle using a photomultiplier tube. A lowpass filter as well as a bandpass filter were used to isolate the second harmonic from the pump beam. Note that because we used an ultrafast laser, the interpretation of our Maker Fringe waveforms differs from a typical Maker fringe measurement. The spatial extent of the femtosecond pulses is much smaller than the thickness of our samples. Therefore, the spatial overlap between the bound and the free second harmonic waves, which travel at different group velocities, decreases drastically as the two wave packets traverse the thickness of the sample [18]. The incomplete overlap results in a reduced interference between the two wave packets, and severely damps the fringes in the Maker fringe envelope. This is particularly relevant to the measurement done on samples where the nonlinearity extends over thicknesses longer than the coherence length in silica (11.9 μm at 800 nm). In a standard Maker fringe experiment with a nanosecond laser source this nonlinearity profile would have resulted in significant modulation fringes, while in our case the fringes are invisible due to the reduced interaction between the free and the bound second harmonic waves. Since a complete theory for Maker fringe SHG with ultrafast pulses is not yet available, we have not been able to quantify the absolute values of the nonlinear susceptibility in our samples. For this reason we present comparative measurements with a bulk fused silica sample thermally poled using the optimal poling conditions as reported in the literature [4].

3. Experimental results and discussion

In the first part of this work, we investigate stacks that consist of a few micrometer-scale layers to study the effect of glass interfaces on the poling-induced nonlinearity. In the second part, we explore the enhancement in the induced nonlinear effect that can be achieved by splitting a micrometer-scale deposited stack into a large number of nanolayers. All the multilayered structures studied here include only commonly used dopants and are fabricated using standard microfabrication techniques, and thus are fully compatible with planar lightwave circuit technology.

To serve as a baseline for comparison, in our first experiment we poled a bulk fused silica sample (a pristine Suprasil 300 substrate; see sample B in Fig. 2). Figure 3 shows the SHG in sample B as a function of the angle between the pump beam and the sample normal. Since Maker fringe measurements do not yield a unique profile of the induced nonlinearity [19], we etched localized regions in the poled sample to study the $\chi^{(2)}$ distribution. Consistent with previous reports on Suprasil glass [15], the etching experiments on sample B showed a long nonlinearity tail that spanned tens of micrometers.

Our initial design of multilayered silica-based structures involved four alternating layers of germanium-doped and undoped layers (see sample G in Fig. 2). The composition of the doped films, as indicated in Fig. 2, was obtained by energy-dispersive x-ray spectroscopy. Note that the introduction of interfaces breaks the symmetry of the glass structure, and thus a non-zero second harmonic signal can be expected in these samples even without poling. Therefore, prior to poling, the SHG in all of the multilayered structures was measured, but was found to be more than two orders of magnitude lower than the SHG in the poled sample B. After the poling process, the measurements of the SHG in sample G showed a factor of two enhancement in the second harmonic signal relative to sample B (Fig. 3).
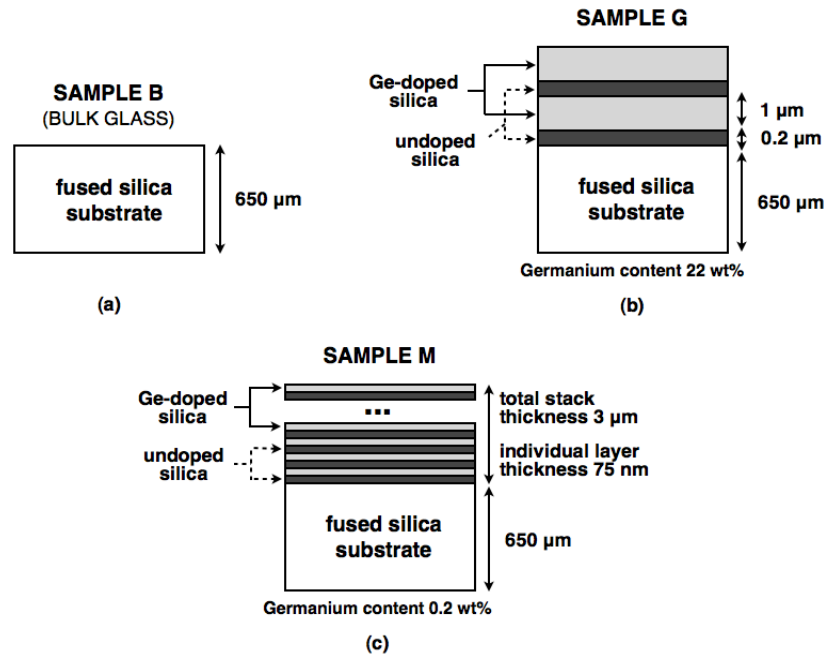
Fig. 2. Thermally poled silica-based samples studied in this work. (a) A bulk glass sample. (b) A four-layered stack of alternating undoped and germanium-doped layers. (c) A multilayered stack consisting of a large number of alternating undoped and germanium-doped nanolayers.
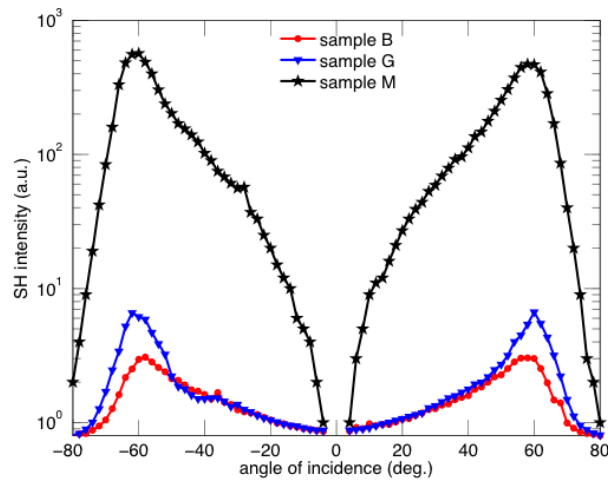

Fig. 3. SHG in thermally poled bulk silica glass and our silica-based multilayered structures. A two-fold SHG enhancement is obtained in sample G compared to sample B, where the two samples were poled under identical conditions. A 204-fold enhancement is obtained in sample M, which consisted of a 3 μm-thick stack with a large number of sub-100 nm-thick nanolayers.

In the second part of our research, we studied multilayered samples that had a total stack thickness of 1.5 to 5 μm, and consisted of a large number of 75 nm-thick silica layers. Although PECVD is generally not designed for the deposition of very thin layers because of its relatively high deposition rate, our system was capable of depositing sub-100 nm-thick alternating layers of undoped and lightly germanium-doped silica. When a sample with 40 nanolayers and 3 μm total stack thickness (see sample M in Fig. 2) was poled, a 204-fold

improvement in the generated second harmonic signal compared to poled bulk glass was observed (Fig. 3).

The preceding discussion compares the SHG in our multilayered samples with the SHG in Suprasil glass. Although previous reports showed that the SHG in Suprasil is one order of magnitude lower than in other silica glasses [4], it is important to note that the SHG in our multilayered stacks is still more than an order of magnitude higher than in even the best bulk fused silica glasses. This result clearly indicates that the idea of poled multilayers can be used as a design strategy towards the realization of a thick silica-based nonlinear region. Further improvements in the induced nonlinearity are expected by optimizing design variables such as the layer deposition technique, the parameters of the multilayered stack, and the poling conditions. For instance, we studied variations of sample M with multilayered stacks of varying thicknesses (Fig. 4), and the results indicate that the large SHG in these structures can be optimized through the design of the multilayered region.

To study the spatial extent of the nonlinearity in sample M as a function of depth, we performed etching experiments in dilute hydrofluoric acid on localized areas of the sample. After each etch, the SHG in the remaining thickness of the sample was remeasured, with the results summarized in Fig. 5. The nonlinearity is located predominantly (>95%) in the multilayered stack, which confirms our hypothesis that silica layers can be used to achieve a high degree of control over the thickness and the location of the $\chi^{(2)}$. We also expect the PECVD process to offer tighter control over impurities in the deposited layers than the flame hydrolysis process that is used to manufacture synthetic silica glass, where the impurity levels may vary significantly between different ingots [15]. Therefore, the amount of impurities that participate in the poling process in our multilayered structures is expected to be consistent between devices that are fabricated at different times, which leads to improved reproducibility, and allows a controlled introduction of dopants into the multilayered structure as a means of enhancing the induced nonlinearity.
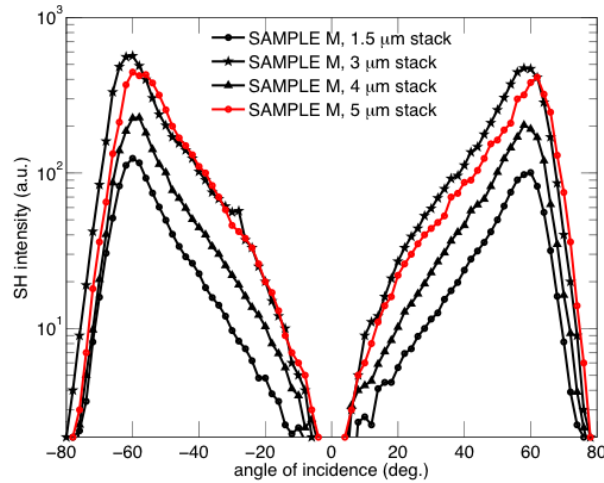

Fig. 4. SHG in thermally poled multilayered structures with varying total stack thicknesses ranging from 1.5 to 5 μm (with the individual layer thicknesses remaining at 75 nm for all samples).
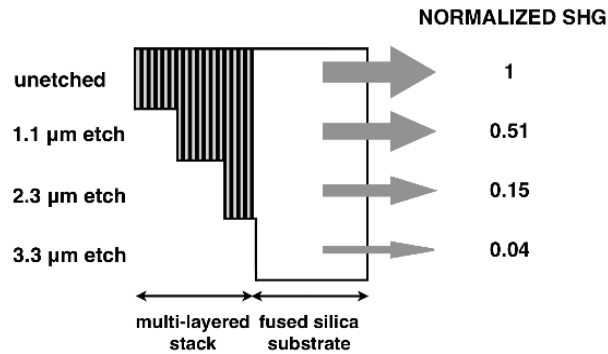
Fig. 5. Remaining SHG in etched thermally poled multilayered structure. Over 95% of the SHG in sample M is concentrated in the 3 μm-thick multilayered stack.

When germanium is introduced into the silica glass matrix, it substitutes for Si^{4+} in the SiO_4 tetrahedra. Unlike other dopants, germanium incorporates into the lattice without any charge-compensating ions because it has the same number of valence electrons as silicon [20]. The enhanced nonlinearity in samples G and M is therefore likely due to a combination of a few factors. First, defects at the interfaces between the germanium-doped and undoped silica act as barriers against the migration of the positive charges, an effect that is consistent with previous observations in poled fibers [21]. These barriers can be advantageous in one of two ways: (1) the accumulation of alkali impurity ions in the vicinity of the interfaces may create strong localized nonlinearity peaks; or (2) the barriers prevent the detrimental positive ions that are injected from the anode from moving further into the sample. We suspect that the two pairs of layers in sample G do not block charge migration as well as the multiple interfaces in sample M [22], which may explain the shape difference (in addition to the magnitude difference) between the Maker fringe patterns of these two samples in Fig. 3. Second, experiments have shown that silica glass with germanium content less than 0.1 mole% (as is the case in sample M) has a lower ionic conductivity compared to undoped silica [23], which furthers slow down any positive charges that may have overcome the interface barrier. And third, when doped with germanium, the refractive index of silica glass increases, thus raising its $\chi^{(3)}$ and in turn the induced effective $\chi^{(2)}$ [22]. A further increase in the $\chi^{(3)}$ of germanium-doped layers may also occur during the poling process [24].

Is the large nonlinearity enhancement observed here limited to layers with germanium-doped silica? We do not believe that this is the case. Our results suggest that the presence of interfaces is the most important factor, and thus it is likely that an enhancement in the SHG will also be observed in multilayered structures with different dopants. In our previous work on corona poled structures with thick layers of phosphorus- and boron-doped silica [25], we showed that a 14-fold increase was obtained in the SHG in phosphorus-doped structures but very little improvement was observed in similar boron-doped structures, which clearly indicates that design optimizations are possible. The use of multilayered structures with glasses that have a large intrinsic $\chi^{(3)}$ (for instance, lead glass [16]) may also yield interesting results. However, to observe the enhanced effect in germanium-doped glass is encouraging since it is the dominant material for the fabrication of low-loss waveguides and fibers. Moreover, the higher refractive index of germanium-doped films raises the average refractive index of the stack, which creates a planar waveguide structure in which an optical mode could be guided, achieving maximum overlap with the nonlinear region that is localized within the stack. Although here we study only planar structures, the same idea can be extended to cylindrical waveguiding structures. An optical fiber with a multilayered silica-based core, where the multilayered design is realized during the fiber preform preparation process, can be thermally poled as illustrated in Fig. 6 by making use of in-fiber electrodes running parallel to the core [26, 27], thereby realizing a second-order nonlinear fiber.
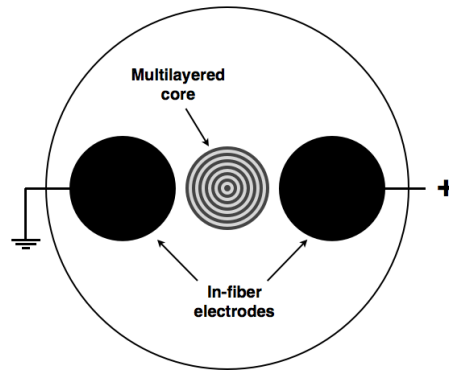
Fig. 6. A conceptual setup for the realization of an efficient second-order nonlinear fiber by thermal poling of a multilayered silica-based core.

7. Conclusion

In conclusion, thermal poling of multilayered silica-based structures was shown to produce a 204-fold enhancement in the induced nonlinearity compared to poled bulk silica glass. This new scheme to create relatively thick, well-controlled nonlinear regions may be further enhanced by the optimization of the thermal poling conditions for the multilayered glass structures. This approach has far-reaching implications for the design of practical silica-based devices with second-order optical nonlinearities, where the doped layers are used as building blocks to create highly customizable artificially created nonlinear materials. Some of the most prominent applications that could benefit from such engineered silica glass nonlinear materials include: (1) all-silica monolithic integration of electro-optic switches and modulators in the PLC platform (as an alternative for the multi-material systems that are in use today); (2) frequency doubling of rare-earth doped fiber lasers to create rugged and inexpensive lasers in the visible spectral region; (3) frequency doubling of high-power pulsed lasers (without concern for damage owing to the high optical damage threshold of silica); and (4) realization of an all-fiber monolithic single-photon source for quantum cryptography applications. The results presented in this paper give a strong indication that the multilayered approach is the key to overcoming the existing challenges of poled glass devices, thus opening the door to practical implementations of efficient active devices in silica glass.

Acknowledgments